

Anisotropic response of spin susceptibility in the superconducting state of UTe_2 probed with ^{125}Te -NMR measurement

Genki Nakamine,¹ Katsuki Kinjo¹, Shunsaku Kitagawa,¹ Kenji Ishida,¹ Yo Tokunaga,² Hironori Sakai,² Shinsaku Kambe,² Ai Nakamura,³ Yusei Shimizu³, Yoshiya Homma,³ Dexin Li,³ Fuminori Honda,³ and Dai Aoki^{3,4}

¹Department of Physics, Kyoto University, Kyoto 606-8502, Japan

²ASRC, Japan Atomic Energy Agency, Tokai, Ibaraki 319-1195, Japan

³IMR, Tohoku University, Oarai, Ibaraki 311-1313, Japan

⁴University Grenoble, CEA, IRIG-PHERIQS, F-38000 Grenoble, France

 (Received 27 October 2020; revised 1 March 2021; accepted 1 March 2021; published 17 March 2021)

To investigate spin susceptibility in a superconducting (SC) state, we measured the ^{125}Te -NMR Knight shifts at magnetic fields (H) up to 6.5 T along the b and c axes of single-crystal UTe_2 , a promising candidate for a spin-triplet superconductor. In the SC state, the Knight shifts along the b and c axes (K_b and K_c , respectively) decreased slightly, and the decrease in K_b was almost constant up to 6.5 T. The reduction in K_c decreased with increasing H , and K_c was unchanged through the SC transition temperature at 5.5 T, excluding the possibility of spin-singlet pairing. Our results indicate that spin susceptibilities along the b and c axes slightly decrease in the SC state in low H , and the H response of SC spin susceptibility is anisotropic on the bc plane. We discuss the possible \mathbf{d} -vector state within the spin-triplet scenario and suggest that the dominant \mathbf{d} -vector component for the case of $H \parallel b$ changes above 13 T, where T_c increases with increasing H .

DOI: [10.1103/PhysRevB.103.L100503](https://doi.org/10.1103/PhysRevB.103.L100503)

Newly discovered UTe_2 with an orthorhombic structure has attracted increasing attention owing to its unusual superconducting (SC) properties [1,2]. It can exhibit superconductivity at magnetic fields (H) that are much higher than the Pauli-limiting field, which can be calculated from the SC transition temperature T_c , and H -boosted superconductivity appears when $H \parallel b$ [1,3]. A novel reentrant superconductivity was also reported for a case when H was applied at a certain angle to the bc plane [4]. Although no ferromagnetic ordering was observed near the SC phase in UTe_2 , such robustness of superconductivity against H seems to be a common feature in uranium-based ferromagnetic and nearly ferromagnetic superconductors [5]. In addition, pressure measurements revealed multiple SC phases [6–9], which can be tuned by H [9,10] and a presumably magnetic ordered phase above 1.8 GPa [8,9,11]. Furthermore, spontaneously broken time-reversal symmetry as revealed from the Kerr measurement [12] and the presence of the chiral Majorana edge and surface state as observed using scanning tunneling spectroscopy [13] were suggested. UTe_2 is like a “toy box” for condensed-matter physicists as it stores most of fascinating topics at present.

In a previous study [14], we reported that UTe_2 is classified as an unconventional superconductor because of the absence of a coherence peak just below T_c ; moreover, the small decrease in the Knight shift when $H \parallel b$, which is much smaller than the expected decrease in a spin-singlet superconductor, is favorable for a spin-triplet scenario because the large spin component remains in the SC state. Similar Knight-shift behaviors were also observed in UPt_3 [15,16] and UCoGe [17,18]. To ensure spin-triplet superconductivity, it is important to identify the spin state of the SC state. For this

purpose, UTe_2 is one of the most suitable superconductors to study physical properties of spin-triplet pairing because superconductivity emerges from the paramagnetic state without the effect from the ordered state.

Spin-triplet superconductivity possesses spin degrees of freedom, which can be expressed as the \mathbf{d} vectors perpendicular to the spin components of the spin-triplet pairing [19]. If the \mathbf{d} vector is fixed to one of the crystalline axes by some mechanism, the spin part of the Knight shift decreases in the SC state when the magnetic-field \mathbf{H} is parallel to the \mathbf{d} -vector ($\mathbf{H} \parallel \mathbf{d}$); however, it remains unchanged in the case of $\mathbf{H} \perp \mathbf{d}$. The \mathbf{d} -vector component can be derived from the measurements of the Knight shift along each crystalline axis. In the previous study, we performed NMR measurements in $H \parallel b$ on the single-crystal sample prepared using a natural tellurium source with 7.1% ^{125}Te , which is a NMR-active isotope. To identify the spin state thoroughly, NMR measurements when $H \parallel c$ and $H \parallel a$ are needed. However, the NMR intensity when $H \parallel c$ was not sufficient to obtain reliable results as the NMR spectrum in $H \parallel c$ is broader than that in $H \parallel b$. This is because of the larger spin susceptibility in the c axis than that in the b axis at low temperatures. Thus, in the present Letter we used a ^{125}Te -enriched single-crystal sample that contained 99.9% of ^{125}Te . This ensured more reliable NMR measurements because the signal intensity of the present sample was roughly one order of magnitude larger than that of the previous sample.

Herein, we report the H dependence of the Knight shift in the SC state along the b and c axes since the NMR spectrum when $H \parallel a$ could not be observed below 20 K due to the divergence of the nuclear spin-spin relaxation rate $1/T_2$

[20]. The findings by the present measurements support the existence of spin-triplet pairing and reveal that the \mathbf{d} vector includes the \hat{b} and \hat{c} components that show an anisotropic response against H on the bc plane.

Single-crystal UTe_2 was grown using the chemical transport method with iodine as the transport agent. Natural uranium and ^{125}Te -enriched metals were used as starting materials for the present sample. The ^{125}Te ($I = 1/2$, gyromagnetic ratio $^{125}\gamma_n/2\pi = 13.454$ MHz/T)-NMR measurements were performed on a single crystal of size $3.5 \times 0.7 \times 1.4$ mm³. The frequency-swept NMR spectrum was obtained using the Fourier transform (FT) of a spin-echo signal observed after the spin-echo radio-frequency pulse sequence with a 3-kHz step in a fixed magnetic field. The magnetic field was calibrated using the ^{65}Cu ($^{65}\gamma/2\pi = 12.089$ MHz/T) NMR signal from the NMR coil. The NMR spectrum in the SC state was recorded with the field-cooling process. We used the split SC magnet, which generated a horizontal field, and combined it with a single-axis rotator to apply a magnetic field exactly parallel to the b or c axis; the a axis was the rotation axis. Low-temperature NMR measurements down to 70 mK were performed using a ^3He - ^4He dilution refrigerator, and the single-crystalline sample was immersed into the mixture. The AC susceptibility was measured by recording the resonance frequency of the NMR-tank circuit during cooling to determine the T_c value of the sample under H .

UTe_2 exhibits two crystallographically inequivalent Te sites $4j$ and $4h$ with point symmetries $mm2$ and $m2m$, respectively. We denote these sites as Te(1) and Te(2), respectively, as shown in Fig. 1(a). The T_c of the present sample determined by the AC susceptibility measurement was consistent with the previous results as shown in Fig. 1(b) [2,3]. Figures 1(c) and 1(d) show the frequency-swept NMR spectrum measured at 3 T when (c) $H \parallel b$ and (d) $H \parallel c$, respectively. The Te(1) and Te(2) signals were distinct when $H \parallel b$ but overlapped when $H \parallel c$. Thus, the Te(2) signal was recorded when $H \parallel b$, and the broad peak consisting of the Te(1) and Te(2) signals was recorded when $H \parallel c$ for the Knight-shift and linewidth measurements. The Knight shift at the Te(2) site was determined from the spectral-peak frequency because the contribution of the Te(2) site was dominant even in the broad spectrum when $H \parallel c$.

Figures 2(a) and 2(b) indicate the NMR spectra measured at several temperatures at 3 T in (a) $H \parallel b$ and (b) $H \parallel c$, respectively, which are shown against $K \equiv (f - f_0)/f_0$. Here, f is the NMR frequency, and f_0 is the reference frequency determined as $f_0 = (\gamma_n/2\pi)H$. Both spectra widen from just below T_c as shown in the Supplemental Material [22], which ensures that the NMR spectrum in the SC state was measured. In addition, shoulder peaks appear in the $H \parallel b$ spectrum below 0.9 K. Because this may suggest the presence of multiple SC phases in H , the origin of the shoulder peaks must be thoroughly investigated. In this Letter, we focus on the temperature variation of the central peak, and the details of the shoulder peaks will be summarized in a separate study. Notably, the main peak of the $H \parallel b$ spectrum, depicted with an arrow, shifts in the SC state, which is visible as a shift from the dotted line showing the normal-state Knight shift. In contrast, the peak of the $H \parallel c$ spectrum, shown by an arrow, slightly shifts in the SC state at 3 T [Fig. 2(b)]; however, the shift

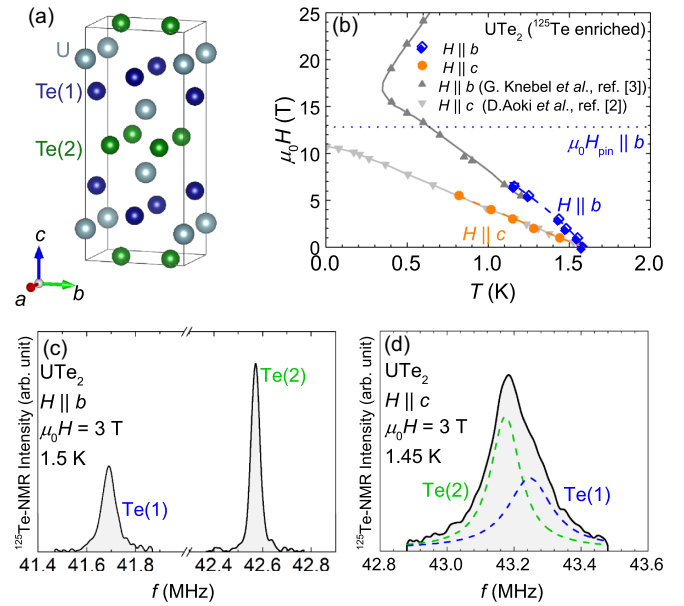


FIG. 1. (a) Image of the crystal structure of UTe_2 prepared with the program VESTA [21]. (b) Upper critical field H_{c2} for a magnetic field applied along the b (diamonds) and c (circles) axes. The solid circles denote T_c of the ^{125}Te -enriched sample, which is consistent with previous results [2,3]. The dotted line indicates the \mathbf{d} -vector pinning field H_{pin} for $H \parallel b$ estimated from the decrease in K_b and $A_{\text{hf},b}$. (c) and (d) ^{125}Te NMR spectra measured when (c) $H \parallel b$ and (d) $H \parallel c$, respectively. The dotted peaks show signals from the Te(1) and Te(2) sites, which are simulated with the resonance frequencies estimated from the angle dependence of the spectrum shown in the Supplemental Material [22].

of the peak could not be recognized in the $H \parallel c$ spectrum measured at 5.5 T, although the broadening of the spectrum was observed in the SC state [Fig. 2(c)]. Subsequently, K_i ($i = b$ and c) is determined by the peak frequencies shown by the arrows.

We investigated the temperature variation of K_b and K_c measured at several magnetic fields below 5.5 T. Figures 3(a)

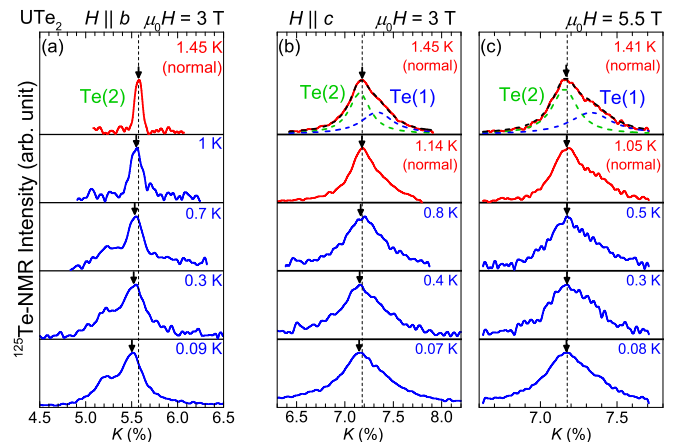


FIG. 2. NMR spectra at several temperatures at 3 T along the (a) b and (b) c axes. NMR spectra at 5.5 T along the (c) c axis. The dotted lines in each figure represent the normal-state peak position.

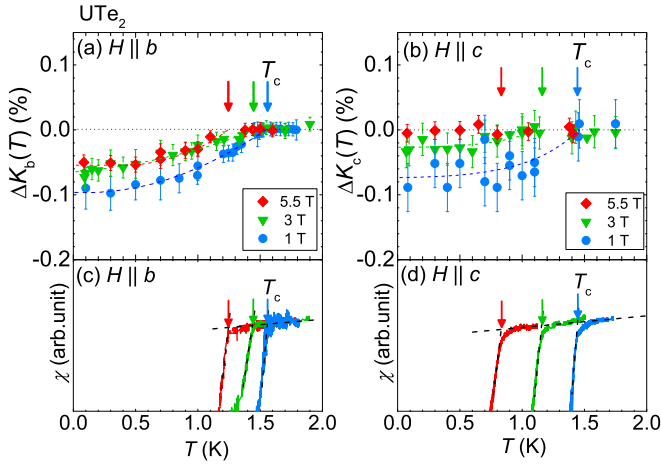


FIG. 3. Temperature dependence of (a) ΔK_b and (b) ΔK_c measured at 1, 3, and 5.5 T (see the text). Dashed lines are added as a guide to the eye. Temperature dependence of the AC susceptibility χ at the same magnetic fields along the (c) b and (d) c axes. The errors of the NMR Knight shift are determined from the resolution of FT signals.

and 3(b) represent the temperature variation of (a) $\Delta K_b(T)$ and (b) $\Delta K_c(T)$ at $\mu_0 H = 1, 3,$ and 5.5 T, which are compared with the temperature dependence of the AC susceptibility. Here, $\Delta K_i(T)$ ($i = b$ and c) is defined as $\Delta K_i(T) \equiv K_i(T) - K_{n,i}$ with the normal-state Knight shift denoted as $K_{n,i}$. The decrease in $\Delta K_b(T)$ observed at 1 T is $\sim 0.1\%$, which is consistent with the previous result [14] and the recent theoretical calculation based on the spin-triplet state [23]. Further reductions at a low temperature, related to the multigap properties, were not observed in the present sample as well as in the previous sample. Notably, the decrease observed at 1 T is almost the same in ΔK_b and ΔK_c . The decreases in $\Delta K_b(T)$ at 3 and 5.5 T in the SC state, which are slightly smaller than that at 1 T, appear to be inconsistent with the previous result [14]. This could be due to the fitting of the whole spectrum for the estimation of the Knight shift in the previous measurement on the ^{125}Te natural-abundant sample. The decrease in ΔK_b in the SC state seems to be almost H independent above 3 T. In contrast, ΔK_c at the lowest temperatures became zero with an increase in H as shown in Fig. 3(b).

To observe the H dependence of the K_i decrease in the SC state more quantitatively, ΔK_i at the lowest temperature (~ 0.1 K), $\Delta K_i(\sim 0.1$ K) is plotted against H in Fig. 4. In general, ΔK_i is attributed to two contributions: a decrease in the spin part of K_i ($\Delta K_{\text{spin},i}$) in the SC state and the SC diamagnetic shielding effect $\Delta K_{\text{dia},i}$, which is expressed as [24]

$$\Delta K_{\text{dia},i} = \frac{H_{c1,i}}{H} \ln \left(\frac{\beta d}{\sqrt{e\xi}} \right). \quad (1)$$

Here, ξ is the Ginzburg-Landau coherence length; β is a factor depending on the vortex structure, is 0.38 for the triangular vortex lattice, and d is the distance between vortices and is calculated using the relation $\phi_0 = \frac{\sqrt{3}}{2} d^2 (\mu_0 H)$. We estimate the H dependence of $\Delta K_{\text{dia},i}$ ($i = b$ and c) as follows: In the estimation of $\Delta K_{\text{dia},c}$, we use the SC critical field (H_c)

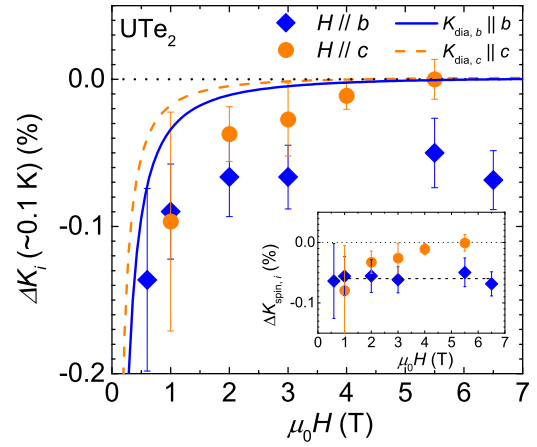


FIG. 4. The magnetic-field dependence of the decrease in ΔK_b (diamonds) and ΔK_c (circles). The solid and dashed lines represent the calculated SC diamagnetic shielding effects $\Delta K_{\text{dia},b}$ and $\Delta K_{\text{dia},c}$, respectively. The inset shows the H dependence of the decrease in $K_{\text{spin},i}$ ($\Delta K_{\text{spin},i}$) estimated by subtracting $\Delta K_{\text{dia},i}$ from ΔK_i .

of UTe_2 , which is reported to be 49 mT [25], and the upper critical field (H_{c2}) along the c axis, which is ~ 11 T as shown in Fig. 1(b). This gives $\mu_0 H_{c1,c} = 1.2$ mT, $\xi = 5.38$ nm, and $\kappa = 159$, and the H dependence of $\Delta K_{\text{dia},c}$ is shown by the dashed curve in Fig. 4. For the estimation of $\Delta K_{\text{dia},b}$, we refer to $\mu_0 H_{c1} = 2$ mT [25], and H_{c2} along the b axis is assumed to be ~ 17 T from the extrapolation of H dependence of T_c in the low- H region. The H dependence of $\Delta K_{\text{dia},b}$ is indicated by the solid curve in Fig. 4. As highlighted by Paulsen *et al.*, the H_{c1} value along the b axis is unexpectedly large and is two times the estimated value from H_c [25]. Even if such an unexpectedly large H_{c1} is adopted for $H \parallel b$, the observed H dependence of the K_b decrease cannot be explained solely based on the H dependence of $\Delta K_{\text{dia},b}$; however, it indicates that K_{spin} along the b and c axes decreases in the SC state, and the decrease in K_{spin} shows an anisotropic response against applied H as shown in the inset of Fig. 4. This suggests that the decrease in the spin susceptibility is maintained, at least, up to 6.5 T when $H \parallel b$; in contrast, it gradually becomes small when $H \parallel c$, and the spin susceptibility remains unchanged with temperature at 5.5 T.

We discuss the plausible SC state based on the present experimental results. As mentioned earlier, the SC pairing in UTe_2 , at least, at ambient pressure, has been considered to be a spin-triplet state. K_c remains unchanged with temperature in the SC state at 5.5 T; this excludes the possibility of spin-singlet pairing even though vortex and/or the H -induced quasiparticle contribution is considered. This is because the decrease in the spin susceptibility should be observed in all directions for spin-singlet pairing. This further supports the spin-triplet scenario. With regard to the spin-triplet superconductivity with odd parity, the possible SC order parameters were highlighted from an ordinary classification theory with D_{2h} point-group symmetry, which are shown in Table I [26]. Since no indication of nonunitary states was observed just below T_c in our measurements, nonunitary states are not considered below. The spin susceptibility decreases with a similar magnitude for $H \parallel b$ and $H \parallel c$ in low H ; this suggests that

TABLE I. Classification of odd-parity SC order parameters for point groups with D_{2h} [26].

Irreducible representation	Basis function
A_u	$k_a\hat{a}, k_b\hat{b}, k_c\hat{c}$
B_{1u}	$k_b\hat{a}, k_a\hat{b}$
B_{2u}	$k_a\hat{c}, k_c\hat{a}$
B_{3u}	$k_c\hat{b}, k_b\hat{c}$

the \mathbf{d} vector contains finite \hat{b} and \hat{c} components in low H . If the strong Ising anisotropy along the a axis in the normal-state spin susceptibility is considered, the \mathbf{d} vector is expected to be perpendicular to the a axis; thus, the B_{3u} state is a promising candidate. This seems to be consistent with the point-node gap suggested by angle-resolved specific-heat measurements [27]. However, because the relationship between the normal-state spin and the \mathbf{d} -vector anisotropy is not clear at present, the A_u state might also be possible. In this case, the component of each basis is highly anisotropic in the \mathbf{k} space. To distinguish the two possibilities, the Knight-shift measurement along the a axis would provide important information regarding the \hat{a} component if it can be measured.

Furthermore, the anisotropic response of the SC spin susceptibility on the bc plane against the applied H suggests that the \hat{c} component in the \mathbf{d} vector becomes small when $H \parallel c$ and is nearly zero at 5.5 T; moreover, the \hat{b} component is robust for $H \parallel b$, thus, indicating that the \mathbf{d} vector is strongly pinned along the b axis. Thus, we consider that the characteristic feature of the low- H SC state is the suppression of the spin susceptibility in $H \parallel b$ (the presence of a finite \hat{b} component in the \mathbf{d} vector). If so, this SC state can sustain up to H_{pin} and a new SC state sets in above H_{pin} where the \mathbf{d} vector is perpendicular to the b axis and $\Delta K_b = 0$. The value of H_{pin} can be estimated from the balance between the SC condensation energy of the low- H superconductivity ($\mu_0 H_c^2/2$) and the Zeeman energy at H_{pin} ($\frac{1}{2}\mu_0 \Delta \chi_b H_{\text{pin}}^2$). A similar discussion was also performed for the ferromagnetic superconductor UCoGe [28]. H_{pin} is estimated to be ~ 13 T from the decrease in spin susceptibility along the b axis $\Delta \chi_b$ derived from the relation $\Delta \chi_b = \Delta K_{\text{spin},b}/A_{\text{hf},b}$ with $\Delta K_{\text{spin},b} \sim 0.060\%$. Here, $A_{\text{hf},b}$ is a hyperfine coupling constant along the b axis, which was reported as $A_{\text{hf},b} = 5.18$ (T/ μ_B) from the K - χ plot in the normal state [20]. Notably, this H_{pin} is close to the critical field

of H_{c2} at which T_c is minimum in H and increases with H as shown in Fig. 1(b). The H -boosted superconductivity might be interpreted as a different SC state where the \mathbf{d} vector can rotate away from the b axis.

Recently, Ishizuka and Yanase calculated the maximum magnitude of intrasublattice \mathbf{d} -vector components in the whole momentum space. They showed that the predominant \mathbf{d} -vector components for the B_{3u} and A_u are $k_b\hat{c}$ and $k_b\hat{b}$, respectively, and these two states are almost degenerate [29]. Thus, one interesting scenario to interpret the anomalous H_{c2} behavior in $H \parallel b$ is that the low- H (high- H) superconductivity corresponds to the A_u (B_{3u}) state, and the \mathbf{d} -vector rotation occurs at approximately 13 T. To verify this case, the Knight-shift measurement above 13 T in $H \parallel b$ is also crucial, and we expect the K_b decrease to become smaller above 13 T and the K_b to remain unchanged in the high- H SC state.

In conclusion, we performed ^{125}Te -NMR on a single crystal of ^{125}Te -enriched UTe₂ and measured the NMR Knight shift when $H \parallel b$ and $H \parallel c$ below T_c . A slight decrease was observed in both K_b and K_c at low H ; however, K_c remained unchanged at 5.5 T between the SC and the normal state. The latter further supports the spin-triplet scenario, and the former indicates the finite components of \hat{b} and \hat{c} in the SC \mathbf{d} vector. From the detailed H dependence, although the \hat{c} component is gradually suppressed when $H \parallel c$, the \hat{b} component is finite, at least, up to 6.5 T, indicating that the \mathbf{d} vector is pinned along the b axis. From the estimation of the pinning field H_{pin} , we suggest that the SC character would be different between the low- H and the high- H SC phases, particularly, about the dominant \mathbf{d} -vector direction. Further experiments to identify the spin state in the high- H SC state and to clarify the origin of the shoulder peaks in $H \parallel b$ are needed and are now in progress.

We would like to thank M. Manago, J. Ishizuka, Y. Yanase, Y. Maeno, S. Yonezawa, and J.-P. Brison, G. Knebel, and J. Flouquet for valuable discussions. This work was supported by the Kyoto University LTM Center, Grants-in-Aid for Scientific Research (Grants No. JP15H05745, No. JP17K14339, No. JP19K03726, No. JP16KK0106, No. JP19K14657, No. JP19H04696, No. JP19H00646, and No. JP20H00130) and Grant-in-Aid for JSPS Research Fellow (Grant No. JP20J11939) from JSPS.

- [1] S. Ran, C. Eckberg, Q.-P. Ding, Y. Furukawa, T. Metz, S. R. Saha, I.-L. Liu, M. Zic, H. Kim, J. Paglione, and N. P. Butch, *Science* **365**, 684 (2019).
- [2] D. Aoki, A. Nakamura, F. Honda, D. Li, Y. Homma, Y. Shimizu, Y. J. Sato, G. Knebel, J.-P. Brison, A. Pourret, D. Braithwaite, G. Lapertot, Q. Niu, M. Valiska, H. Harima, and J. Flouquet, *J. Phys. Soc. Jpn.* **88**, 043702 (2019).
- [3] G. Knebel, W. Knafo, A. Pourret, Q. Niu, M. Valiska, D. Braithwaite, G. Lapertot, M. Nardone, A. Zitouni, S. Mishra, I. Sheikin, G. Seyfarth, J.-P. Brison, D. Aoki, and J. Flouquet, *J. Phys. Soc. Jpn.* **88**, 063707 (2019).
- [4] S. Ran, I.-L. Liu, Y. S. Eo, D. J. Campbell, P. M. Neves, W. T. Fuhrman, S. R. Saha, C. Eckberg, H. Kim, D. Graf, F. Balakirev, J. Singleton, J. Paglione, and N. P. Butch, *Nat. Phys.* **15**, 1250 (2019).
- [5] D. Aoki, K. Ishida, and J. Flouquet, *J. Phys. Soc. Jpn.* **88**, 022001 (2019).
- [6] D. Braithwaite, M. Vališka, G. Knebel, G. Lapertot, J.-P. Brison, A. Pourret, M. E. Zhitomirsky, J. Flouquet, F. Honda, and D. Aoki, *Commun. Phys.* **2**, 147 (2019).
- [7] S. Ran, H. Kim, I.-L. Liu, S. R. Saha, I. Hayes, T. Metz, Y. S. Eo, J. Paglione, and N. P. Butch, *Phys. Rev. B* **101**, 140503(R) (2020).
- [8] S. M. Thomas, F. B. Santos, M. H. Christensen, T. Asaba, F. Ronning, J. D. Thompson, E. D. Bauer, R. M. Fernandes, G. Fabbris, and P. F. S. Rosa, *Sci. Adv.* **6**, eabc8709 (2020).

- [9] D. Aoki, F. Honda, G. Knebel, D. Braithwaite, A. Nakamura, D. Li, Y. Homma, Y. Shimizu, Y. J. Sato, J.-P. Brison, and J. Flouquet, *J. Phys. Soc. Jpn.* **89**, 053705 (2020).
- [10] W.-C. Lin, D. J. Campbell, S. Ran, I.-L. Liu, H. Kim, A. H. Nevidomskyy, D. Graf, N. P. Butch, and J. Paglione, *npj Quantum Mater.* **5**, 68 (2020).
- [11] G. Knebel, M. Kimata, M. Vališka, F. Honda, D. Li, D. Braithwaite, G. Lapertot, W. Knafo, A. Pourret, Y. J. Sato, Y. Shimizu, T. Kihara, J.-P. Brison, J. Flouquet, and D. Aoki, *J. Phys. Soc. Jpn.* **89**, 053707 (2020).
- [12] I. M. Hayes, D. S. Wei, T. Metz, J. Zhang, Y. S. Eo, S. Ran, S. R. Saha, J. Collini, N. P. Butch, D. F. Agterberg, A. Kapitulnik, and J. Paglione, [arXiv:2002.02539](https://arxiv.org/abs/2002.02539).
- [13] L. Jiao, S. Howard, S. Ran, Z. Wang, J. O. Rodriguez, M. Sigrist, Z. Wang, N. P. Butch, and V. Madhavan, *Nature (London)* **579**, 523 (2020).
- [14] G. Nakamine, S. Kitagawa, K. Ishida, Y. Tokunaga, H. Sakai, S. Kambe, A. Nakamura, Y. Shimizu, Y. Homma, D. Li, F. Honda, and D. Aoki, *J. Phys. Soc. Jpn.* **88**, 113703 (2019).
- [15] H. Tou, Y. Kitaoka, K. Asayama, N. Kimura, Y. Ōnuki, E. Yamamoto, and K. Maezawa, *Phys. Rev. Lett.* **77**, 1374 (1996).
- [16] H. Tou, Y. Kitaoka, K. Ishida, K. Asayama, N. Kimura, Y. Ōnuki, E. Yamamoto, Y. Haga, and K. Maezawa, *Phys. Rev. Lett.* **80**, 3129 (1998).
- [17] T. Hattori, K. Karube, Y. Ihara, K. Ishida, K. Deguchi, N. K. Sato, and T. Yamamura, *Phys. Rev. B* **88**, 085127 (2013).
- [18] M. Manago, S. Kitagawa, K. Ishida, K. Deguchi, N. K. Sato, and T. Yamamura, *Phys. Rev. B* **100**, 035203 (2019).
- [19] A. J. Leggett, *Rev. Mod. Phys.* **47**, 331 (1975).
- [20] Y. Tokunaga, H. Sakai, S. Kambe, T. Hattori, N. Higa, G. Nakamine, S. Kitagawa, K. Ishida, A. Nakamura, Y. Shimizu, Y. Homma, D. Li, F. Honda, and D. Aoki, *J. Phys. Soc. Jpn.* **88**, 073701 (2019).
- [21] K. Momma and F. Izumi, *J. Appl. Crystallogr.* **44**, 1272 (2011).
- [22] See Supplemental Material at <http://link.aps.org/supplemental/10.1103/PhysRevB.103.L100503> for the details of the experimental setting and the temperature dependence of the NMR linewidth.
- [23] K. Hiranuma and S. Fujimoto, *J. Phys. Soc. Jpn.* **90**, 034707 (2021).
- [24] P. G. de Gennes, *Superconductivity of Metals and Alloys* (W. A. Benjamin, New York, 1966).
- [25] C. Paulsen, G. Knebel, G. Lapertot, D. Braithwaite, A. Pourret, D. Aoki, F. Hardy, J. Flouquet, and J.-P. Brison, [arXiv:2002.12724](https://arxiv.org/abs/2002.12724).
- [26] J. Ishizuka, S. Sumita, A. Daido, and Y. Yanase, *Phys. Rev. Lett.* **123**, 217001 (2019).
- [27] S. Kittaka, Y. Shimizu, T. Sakakibara, A. Nakamura, D. Li, Y. Homma, F. Honda, D. Aoki, and K. Machida, *Phys. Rev. Research* **2**, 032014(R) (2020).
- [28] Y. Tada, S. Takayoshi, and S. Fujimoto, *Phys. Rev. B* **93**, 174512 (2016).
- [29] J. Ishizuka and Y. Yanase, *Phys. Rev. B* **103**, 094504 (2021).